PRECISE GEOREFERENCING OF CARTOSAT IMAGERY VIA DIFFERENT ORIENTATION MODELS

J. Willneff, T. Weser, F. Rottensteiner, C. S. Fraser *

Cooperative Research Centre for Spatial Information, Department of Geomatics, The University of Melbourne, VIC 3010, Australia - jwillneff@web.de, (tweser, franzr, c.fraser)@unimelb.edu.au

Commission I, SS-11

KEY WORDS: CARTOSAT, high-resolution, satellite, orientation, comparison

ABSTRACT:

The CARTOSAT 1 satellite, launched by the Indian Space Research Organisation (ISRO) in 2005, can provide panchromatic along-track stereo imagery with a ground resolution of 2.5 m. Along with the imagery, encrypted files with rational polynomial coefficients (RPCs) and meta-data are distributed by ISRO. The RPCs allow direct georeferencing within certain limits depending on the on-board systems for registering the orbit path and attitudes of the satellite. At the Cooperative Research Centre for Spatial Information at the University of Melbourne (Australia), the software package *Barista* for the processing of high-resolution satellite images is being developed. *Barista* offers three techniques for precise georeferencing of such image data, namely the 3D affine model, bias correction for RPCs, and a generic pushbroom sensor model. The 3D affine model can only be applied when ground control points (GCPs) are available. The RPC model can be improved beyond the limits of direct georeferencing by correcting for the biases contained in the original RPCs. This process requires at least one well-defined GCP per image. Whereas the meta-data for CARTOSAT 1 imagery do not contain all the information required for using the generic pushbroom sensor model for direct georeferencing, they provide initial values for such a sensor model to be determined if enough GCPs are available. In this paper, the authors compare the geopositioning accuracy achievable with CARTOSAT 1 imagery via the 3D affine, bias-corrected RPC and generic pushbroom sensor models. A stereo pair of images covering Hobart, Australia, was processed using *Barista*. In addition to the imagery, an object point array of altogether 69 3D GPS-surveyed points was utilised. They were distributed all over Hobart and covered about one quarter of the scene. In order to assess the georeferencing accuracy that can be achieved using CARTOSAT 1 images, bundle adjustment was carried out using all three sensor models and nine well-distributed GCPs. The absolute accuracy was then assessed via the remaining 60 points, which served as independent checkpoints. The georeferencing results obtained for CARTOSAT 1 in the Hobart test field are very encouraging. Whereas direct georeferencing using the RPCs provided by ISRO yielded sub-optimal results, the provision of a small number of GCPs is enough to boost the positioning accuracy to subpixel level in planimetry and to make it slightly better than 1 pixel in height, independent from the sensor model used.

1. INTRODUCTION

The number of commercial high-resolution satellites has steadily increased over recent years. The available image products from the current operational satellites have a ground resolution from a few metres to half a metre and are used for the extraction of spatial information for a variety of mapping and GIS applications. For the extraction of metric information from images, suitable sensor orientation models describing the relationship between image space and object space are necessary. This paper describes the application of three different sensor models and the assessment of their accuracy from processing a data set acquired with the CARTOSAT 1 satellite. Launched in 2005 by the Indian Space Research Organisation (ISRO), CARTOSAT 1 can provide panchromatic along-track stereo imagery with a ground resolution of 2.5 m. The radiometric resolution is 10 bit. One option for sensor orientation of CARTOSAT 1 images is a camera replacement model using rational polynomial coefficients (RPCs), comprehensively described in Grodecki and Dial (2001) and Tao and Hu (2002). Along with the imagery, encrypted files with RPCs and meta-data are distributed by ISRO. Certified software distributers will additionally be provided with decryption software for these RPCs so that they can be accessed and used for direct georeferencing of the imagery within certain limits. These limits depend on the accuracy of the on-board systems for registering the orbit path and attitudes of the satellite in order to generate the RPCs from a generic pushbroom scanner model. In the case of CARTOSAT 1, the RPCs provided by ISRO should allow direct georeferencing with an accuracy of about 30 pixels. As the provided metadata contain neither a precise camera calibration nor information about orbit path and attitude angles, direct georeferencing is not possible with a generic pushbroom sensor model.

At the Cooperative Research Centre for Spatial Information (CRC-SI) at the University of Melbourne, Australia, the software package *Barista* for the processing of high-resolution satellite images is being developed to support various research initiatives dealing with the extraction of spatial information. *Barista* offers three techniques for precise georeferencing of satellite images and all require ground control points (GCPs). First, the 3D affine model has been shown in the past to deliver pixel-level results for high-resolution satellite imagery in scenes of limited extent. In this case, no additional information is required from the vendor of the satellite images. Second, bias corrections can be applied to the RPCs provided by ISRO if they can be accessed. These bias corrections can be modelled

* Corresponding author.

either by mere shifts, by shifts and drifts, or by an affine transformation, all in image space. It has been shown in the past that the effect of the biases is almost constant in the images, so that by using one well-defined GCP per image, the bulk of the bias can be removed (Fraser and Hanley, 2003). Results can be improved if a modest number of additional GCPs are available. Third, a generic pushbroom sensor model can be initialized from information contained in the metadata files and refined in an orientation process by the use of well-distributed GCPs. If the metadata of CARTOSAT 1 imagery contained information about the orbit path and attitudes, the generic pushbroom scanner model could also be used for direct georeferencing, and the GCPs could be used for determining biases in the orbit path and attitude information. As this is not the case, the orbit path and attitudes need to be determined from GCPs alone. The number of GCPs required will be slightly higher than would be the case if orbit path and attitude information were available.

In this paper, the authors assess and compare the geopositioning accuracy achievable with CARTOSAT 1 imagery via the 3D affine, bias-corrected RPC and generic pushbroom sensor models. A stereo pair of images covering Hobart, Australia, distributed by ISRO as part of the Cartosat-1 Scientific Assessment Programme (C-SAP), was processed using *Barista*. Unencrypted RPC files were provided by ISRO for research purposes in this case. General information about the satellite can be found in CARTOSAT 1a (2006) and CARTOSAT 1b (2006). Scene related information is contained in the provided metadata files. A set of GPS-surveyed 3D points for the area of Hobart was available for the reported analysis. In order to assess the georeferencing accuracy that can be achieved for CARTOSAT 1 images, bundle adjustment was carried out, applying the three sensor models accommodated within *Barista* and using a subset of the available 3D points as GCPs. The remaining 3D points served as independent check points.

2. THE HOBART DATA SET

2.1 Imagery

For the assessment of the georeferencing accuracy a stereo pair of panchromatic CARTOSAT 1 images was used. The nominal flying height of the satellite is 618 km and the two cameras are mounted with a tilt of +26 degrees (fore) and -5 degrees (aft). Table 1 shows some satellite specifications. Further information can be found in CARTOSAT 1a (2006) and CARTOSAT 1b, (2006). The provided metadata files specified a slightly different value of around 638 km for the flying height. No scene specific across-track angle information is given. The forward scene covers an area of roughly 30 km x 30 km around the city of Hobart. The area covered by the aft view is about 27 km x 30 km. The elevations in this area range from sea level up to over 1260 m at the peak of Mt Wellington. The acquisition date of the Hobart images was 1 October 2006.

2.2 3D Points

In addition to the imagery, a test field of altogether 69 3D points was utilised. This test field is described in Fraser and Hanley (2005). The points were distributed all over Hobart and covered the top left quarter of the scene. They were measured with GPS and were mainly centres of road roundabouts, determined as the centres of ellipses fitted to points around the roundabout perimeter. A selection of 9 points was used to provide GCPs for the bundle adjustment. The absolute accuracy was then assessed via the remaining 60 points, which served as independent checkpoints. For the generic pushbroom sensor model an adjustment was also performed with 15 GCPs and 54 checkpoints in order to investigate the influence of the number of GCPs on the results. Figure 1 shows the CARTOSAT 1 forward-looking scene with the distribution of the 15 GCPs. The 9 GCPs covered the same area but with a less dense point distribution.

Orbital altitude		618 km
Swath	Fore	29.42 km
	Aft	26.24 km
Along-track view angle	Fore	+26 °
	Aft	-5 °
Across-track resolution (at Nadir)	Fore	2.452 m
	Aft	2.187 m
Ground sampling distance (along-track)		2.54 m
B/H ratio		0.62
Image size		12 000 x 12 000
Pixel size		7 x 7 microns
Focal length		1945 mm

Table 1. CARTOSAT 1 specifications.

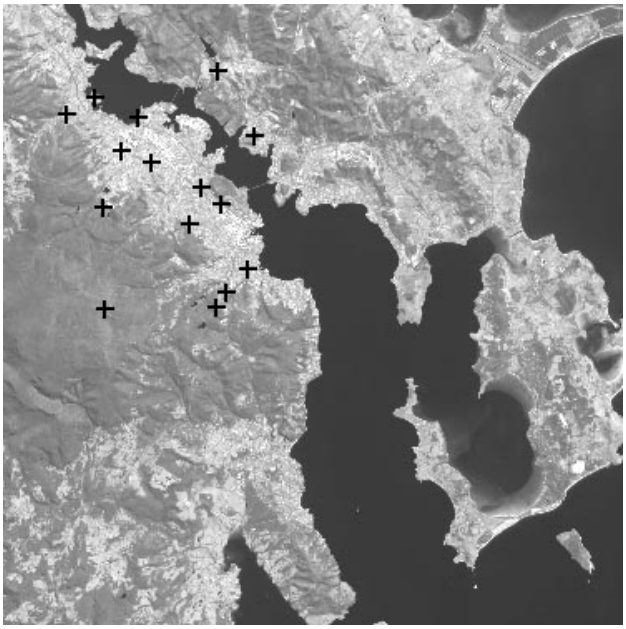

Figure 1. CARTOSAT 1 forward-looking scene of Hobart with 15 GCPs.

3. SENSOR MODELS IN BARISTA

The processing of the CARTOSAT 1 data set of Hobart was carried out with the software system *Barista*. *Barista* is developed at the CRC-SI and has reached the status of a commercially available product. It is a software system for the generation of spatial information products from satellite imagery. Data sets from high-resolution satellites such as QuickBird, WorldView, IKONOS, SPOT 5, and ALOS/PRISM have been processed successfully with *Barista*. Further details about the software can be found in Barista (2008).

In order to exploit the full potential of high-resolution satellite images for 3D information extraction it is essential that precise georeferencing is applied. *Barista* handles three different sensor models for georeferencing to establish the object space to image space transformation and vice-versa.

3.1 3D affine model

The 3D affine model is an approximation of the actual imaging process by a parallel projection (Fraser and Yamakawa, 2004). This approximation is justified by the very narrow fields of view of commercial high-resolution satellites. The model does not explicitly utilise camera or orientation parameters. The transformation relating the 2D image coordinates of a point with its object coordinates is given as

$$\begin{aligned} x &= a_1 \cdot X + a_2 \cdot Y + a_3 \cdot Z + a_4 \\ y &= a_5 \cdot X + a_6 \cdot Y + a_7 \cdot Z + a_8 \end{aligned} \quad (1)$$

with X, Y, Z: object coordinates
x, y: image coordinates
a_i: parameters of 3D affine transformation

The 3D affine model can be applied independently from the type of the object coordinate system; here the adjustments were carried out with the GCPs being defined in geocentric, geographic, and UTM coordinates. The optimal reference coordinate system for the affine model and its assumption of a parallel imaging plane is the UTM projection (Fraser and Yamakawa, 2004). A minimum of 4 non-coplanar GCPs is required to determine the parameters of the 3D affine model.

3.2 RPC sensor model

In the case of the RPC sensor model, a set of rational polynomial coefficients are used as a camera replacement model. They are provided by the image distributors and are known to have a significant bias. This bias can be removed with at least one well-defined GCP (Fraser et al., 2006). The transformation relating the 2D image coordinates of a point with its object coordinates is given as

$$\begin{aligned} x + B_0 + B_1 \cdot y + B_2 \cdot x &= \frac{Num_x(\varphi, \lambda, h)}{Den_x(\varphi, \lambda, h)} \\ y + A_0 + A_1 \cdot y + A_2 \cdot x &= \frac{Num_y(\varphi, \lambda, h)}{Den_y(\varphi, \lambda, h)} \end{aligned} \quad (2)$$

with φ, λ, h: latitude, longitude, and ellipsoidal height
x, y: image coordinates
Num_x, Den_x: cubic polynomial functions of object space coordinates for x
Num_y, Den_y: cubic polynomial functions of object space coordinates for y
A_i, B_i: affine parameters of bias correction.

Note that the (altogether 80) coefficients of the four polynomials in Equation 2 are distributed by ISRO, so that they can be used for direct georeferencing. However, Equation 2 also incorporates the bias correction by an affine transformation in image space. The parameterisation of the bias correction can be changed in *Barista*. The minimum parameterisation of the bias correction is by the two shifts A_0 and B_0; if this parameterisation is chosen, the other parameters will be set to zero, and they will be kept constant in the adjustment. In order to additionally compensate for drift effects, the parameters A_1 and B_1 can be determined. The third option is to determine all the parameters A_i and B_i of the 2D affine transformation. The number of GCPs required depends on the parameterisation: If only shifts are used to model the bias, one well-defined GCP is enough. Two appropriately positioned GCPs is the minimum needed for determining shift and drift parameters, and three GCPs are required for the full affine bias correction model.

3.3 Generic pushbroom sensor model

The generic pushbroom sensor model uses a physical camera model, modelling the orbit path and attitudes by splines. In order to determine the parameters of these splines, direct observations taken from orbit path and attitude recordings provided by the image distributors are used in the adjustment process. Since the definitions of the parameters delivered by different data vendors are not identical and sometimes not even compatible, the vendor-specific data have to be mapped to the model used in *Barista* when these metadata are imported. Such import functions have been implemented for SPOT 5, QuickBird and ALOS. The transformation relating the image point $\mathbf{p}_F$ in the image line coordinate system to the object point $\mathbf{P}_{ECS}$ in the object coordinate system is given as:

$$\mathbf{p}_F - \mathbf{c}_F + \delta\mathbf{x} = \lambda \cdot \mathbf{R}_M^T \cdot \{\mathbf{R}_P^T(t) \cdot \mathbf{R}_O^T \cdot [\mathbf{P}_{ECS} - \mathbf{S}(t)] - \mathbf{C}_M\} \quad (3)$$

with $\mathbf{P}_{ECS}$: point in an earth centred system
$\mathbf{S}(t)$: satellite position at time t, modelled by splines
$\mathbf{R}_O$: time-constant rotation matrix, rotating into a nearly tangential system
$\mathbf{R}_P(t)$: time-dependant rotation matrix depending on three rotational angles *roll(t), pitch(t), yaw(t)*, each of them modelled by a spline function
$\mathbf{C}_M$: position of the camera centre in the satellite (camera mounting)
$\mathbf{R}_M$: rotation matrix from the camera system to the satellite (platform) system
λ: scale factor describing the position of the point along the image ray
$\mathbf{p}_F$: $(x_F, 0, 0)^T$: image coordinates of $\mathbf{P}$ in the image line (framelet) coordinate system
$\mathbf{c}_F$: $(x_{F0}, y_{F0}, F)^T$: position of the projection centre relative to the image line
$\delta\mathbf{x}$: **c**orrections for systematic errors.

Equation 3 has three components. By dividing the first and the second component of the equation by the third, the scale factor λ is eliminated, and the remaining two equations describe a perspective transformation with time-dependant projection centre and rotations. The time t is closely related to and can be determined from the measured y coordinate of a point, i.e. the line index in the digital image; the observed y_F coordinate (the y coordinate in the CCD line) is 0. Both the satellite path $\mathbf{S}(t)$ and the three angles used to compute $\mathbf{R_P}(t)$ are modelled by spline functions. The orbit path and attitude information provided in the metadata files are used as direct observations for determining the parameters of the splines. The sensor model also contains a model for the correction of systematic errors in

these direct observations. Details about the generic pushbroom sensor model can be found in Weser et al. (2007).

In the case of CARTOSAT 1, the metadata delivered with the images do not contain the information required to determine the parameters of the generic pushbroom scanner model, so that it cannot be used for direct georeferencing. However, *Barista* allows the determination of the pushbroom sensor model if at least some metadata plus enough GCPs are available. If the approximate latitude and longitude of the four corners of the image, the flying height of the satellite (H), the focal length, and the approximate look-angles of the camera are known, the pushbroom sensor model can be initialized, and approximate values for its parameters can be determined. In the case of CARTOSAT 1, the values for coordinates of the corners of the image, the flying height and the along-track look-angle are specified in the metadata file distributed with the CARTOSAT 1 imagery. The values for the focal length (1945mm) and the sensor pixel size (7µm) are given in CARTOSAT 1b (2006). Alternatively the focal length can also be coarsely estimated from the flying height and the swath width.

Once approximate values have been determined, the precise values of the parameters of the pushbroom sensor model, i.e., the values of the parameters of the spline functions describing the time-dependant orbit path $\mathbf{S}(t)$ and attitudes $\mathbf{R}_P(t)$, can be determined from GCPs. The parameters of the interior orientation cannot be improved, but this would hardly be possible anyway given the sensor geometry (very small opening angles). Thus, errors in the focal length will be compensated by shifts in the orbit path. The fact that no direct observations for the orbit path and attitudes are available has to be compensated by a larger number of GCPs than would otherwise be required and by modifications to the sensor model. In the following sections, the initialisation of the sensor model parameters and the modifications of the sensor model will be described.

3.3.1 Initializing the approximate parameters of the generic pushbroom sensor model:

To initialize the sensor model, the parameters $\mathbf{c}_F$, $\mathbf{R}_M$, $\mathbf{C}_M$, $\mathbf{R}_P(t)$, $\mathbf{S}(t)$, and $\mathbf{R}_O$ in Equation 3 have to be approximately determined. Using the nominal values for the focal length and the pixel size and assuming the principal point to be in the centre of the image line results in $\mathbf{c}_F = (N/2, 0, f)^T$, where N is the number of pixels in an image line and f is the focal length in pixels. The position $\mathbf{C}_M$ of the camera in the satellite is assumed to be $\mathbf{C}_M=(0,0,0)^T$. These values will be kept constant in the adjustment. All the spline parameters used to model the time dependant angles *roll(t), pitch(t), yaw(t)* parameterising $\mathbf{R}_P(t)$ are also initialised with zero, which yields $\mathbf{R}_P(t)=\mathbf{I}$. This means that the satellite orbit and satellite platform systems (Weser et al., 2007) are initially identical. $\mathbf{R}_M$, the rotation matrix from the camera system to the satellite platform system, can be computed from the along-track viewing angle α and the across-track viewing angle β:

$$\mathbf{R}_M = [\mathbf{X}_M, \mathbf{Y}_M, \mathbf{Z}_M] \quad (4)$$

with $\mathbf{Z}_M = \mathbf{Z}_0 / \| \mathbf{Z}_0 \|$

$\mathbf{Z}_0 = [\tan(\alpha), -\tan(\beta), -1]^T$

$\mathbf{X}_M = [0, \cos(\alpha), -\sin(\beta)]^T$

$\mathbf{Y}_M = \mathbf{Z}_M \times \mathbf{X}_M$

The remaining parameters $\mathbf{S}(t)$ and $\mathbf{R}_O$ cannot be determined separately. $\mathbf{R}_O$ is computed from the satellite position at the scene centre (Weser et al, 2007) whereas $\mathbf{S}(t)$ can only be computed when $\mathbf{R}_O$ is known. This leads to an iterative process in order to determine both parameters.

The centres of the first ($\mathbf{M}_F$) and last ($\mathbf{M}_L$) image rows are determined from the four corner points. Extending the position vectors $\mathbf{M}_F$ and $\mathbf{M}_L$ in geocentric coordinates by the factor $(1 + H/R)$, where R denotes the earth radius, yields two approximate orbit points $\mathbf{S}^0{}_F$ and $\mathbf{S}^0{}_L$. The orbit path is approximated by a circle of radius $R_s = (R + H)$ connecting $\mathbf{S}^0{}_F$ and $\mathbf{S}^0{}_L$ and passing through the earth centre. The first approximation for $\mathbf{R}_0$, namely $\mathbf{R}_0{}^0$, can be determined from this path, as described in Weser et al. (2007). Since this approximation does not yet consider the viewing angles α and β, it has to be improved.

The third column vector of $\mathbf{R}_M$ according to Equation 4, $\mathbf{Z}_M$, describes the viewing direction of the satellite camera in the platform system. Denoting the approximation for $\mathbf{R}_0$ after iteration step i by $\mathbf{R}_0{}^i$, the vector $\mathbf{g}^i$ describing the viewing direction in the geocentric object coordinate system is given by $\mathbf{g}^i = \mathbf{R}_0{}^i \cdot \mathbf{Z}_M$. The improved positions of the orbit end points in iteration $i + 1$ are situated on straight lines parallel to $\mathbf{g}^i$, thus $\mathbf{S}^{i+1}{}_j = \mathbf{M}_j + \lambda_j \cdot \mathbf{g}^i$ with $j \in \{F, L\}$. The intersections of these straight lines with a sphere of radius R_s yield the improved positions $\mathbf{S}^{i+1}{}_F$ and $\mathbf{S}^{i+1}{}_L$, from which improved orbit path parameters and an improved rotation matrix $\mathbf{R}_0{}^{i+1}$ are derived. The iterations cease when the positions of $\mathbf{S}_F$ and $\mathbf{S}_L$ change by less than a pre-defined distance threshold between two successive iterations. Back-projecting the GCPs to the stereo pair using the approximate values determined as described above results in offsets of up to 500 pixels in image space, which is close enough for the bundle adjustment to converge.

3.3.2 Modification of the generic pushbroom sensor model:

The parameters to be determined via bundle adjustment using GCPs are the coefficients of the spline functions used to model the time-dependant orbit path, $\mathbf{S}(t)$, and attitudes, $\mathbf{R}_P(t)$. In Weser et al. (2007), the components of $\mathbf{S}(t)$ and the angles *roll(t), pitch(t), yaw(t)* parameterising $\mathbf{R}_P(t)$ were modelled by cubic splines. In order to reduce the number of parameters to be determined, the degree of the spline functions is reduced to 2 if no direct observations for the orbit path and attitudes are available. Furthermore, additional observations are used in the adjustment to act as 'soft constraints' to achieve a more stable solution for the spline coefficients. First, a fictitious observation of a point to be situated in a plane passing through the earth centre is added for several points along the orbit path, thus forcing $\mathbf{S}(t)$ into such a plane with a certain a priori standard deviation. Second, by direct observations of the position vectors $\mathbf{S}(t)$ and the tangential vectors $d\mathbf{S}(t) / dt$ being perpendicular at several discrete times t, the orbit path $\mathbf{S}(t)$ is forced to be almost circular. The additional observations should keep the number of GCPs required to determine the parameters in the model described by Equation 3 within reasonable limits, without compromising the accuracy of the model.

4. EXPERIMENTS

This section shows the results of the georeferencing obtained by applying the three different sensor models. In each adjustment, the check points were only used as tie points, and their coordinates were determined in the adjustment. The same stochastic model was used in all cases: the a priori standard deviation of an image coordinate was ±0.5 pixels, and the a priori standard deviation of a GCP coordinate was ±0.3 m (or its equivalent in the case of geographic coordinates). The tables in this section show the root mean square (RMS) errors of the differences between the measured image coordinates and the results of back-projecting the original check points for the scenes (RMS_x and RMS_y) for the scenes *Fore* and *Aft*. Furthermore, the RMS errors of object coordinate differences between the results of bundle adjustment and the original check point coordinates (RMS_X, RMS_Y, RMS_Z) are presented along with the minimum and maximum residuals in the object coordinates of the check points (R_X^{min} / R_X^{max}, R_Y^{min} / R_Y^{max}, R_Z^{min} / R_Z^{max}), and the RMS error of the standard error of unit weight s_0 of each adjustment.

4.1 Results using the 3D affine model

The georeferencing results with the 3D Affine model are summarized in Table 2. For this model with 9 GCPs, the RMS values of differences between the measured image coordinates and back-projected coordinates of the checkpoints were between 0.3 and 0.6 pixels. The corresponding RMS errors in object space were below 1.8 m in both planimetry and height. It has been shown that use of GCPs defined in UTM leads to better results than use of GPCs in geographic coordinates (Hanley et al. 2002), which was also the case with this data set. The results achieved for geocentric coordinates and for UTM are very similar, though there is a different distribution of the error budget to the individual components due to the different definitions of X, Y and Z.

System	Geocentric		Geographic		UTM	
Scene	Fore	Aft	Fore	Aft	Fore	Aft
RMS_x [pixel]	0.32	0.32	0.54	0.55	0.33	0.33
RMS_y [pixel]	0.55	0.41	0.56	0.54	0.53	0.42
RMS_X [m]	1.20		1.43		0.80	
R_X^{min}/R_X^{max} [m]	-5.1 / 2.3		-4.0 / 3.5		-1.4 / 2.5	
RMS_Y [m]	0.96		1.17		1.00	
R_Y^{min}/R_Y^{max} [m]	-3.5 / 3.2		-4.0 / 2.8		-4.1 / 2.4	
RMS_Z [m]	1.33		1.81		1.81	
R_Z^{min}/R_Z^{max} [m]	-5.4 / 2.5		-4.3 / 7.0		-4.2 / 7.1	
s_0	0.42		0.53		0.41	

Table 2. Results of georeferencing with the 3D affine model.

4.2 Results using RPCs

First, the accuracy of the original RPCs provided by ISRO was checked by back-projecting the GCPs into the images. It was found that there was an almost constant offset of approximately 33 pixels in both images of the stereo pair. Whereas the offset was almost entirely in the flight direction in the forward looking image, there was both an along-track and a cross-track component in the backward facing image. Computing the 3D coordinates of the GCPs by forward intersection using the original RPCs, and comparing the resulting coordinates with those determined by GPS, resulted in RMS discrepancy values of 72 m in planimetry and 25 m in height. The discrepancies were highly systematic and applying the bias-correction was expected to increase the quality of the results significantly. The results of the forward intersection with the original RPCs are shown in Table 3.

Bundle block adjustment was carried out using the three options of *shift only*, *shift and drift*, and *affine* for the bias compensation of the RPCs. The results achieved using 9 GCPs are shown in Table 4. Determining drift parameters in addition to the shifts results mainly in an improvement of the height accuracy by about 10%. Use of the affine bias correction model resulted in additional improvement in both the height component and the planimetric accuracy. There is also an improvement in the image-based RMS errors. In the case of affine bias correction, the RMS errors of differences were considerably better than the pixel size in all components.

Scene	Fore	Aft
RMS_x [pixel]	0.91	15.92
RMS_y [pixel]	33.27	26.80
RMS_X [m]	2.7	
R_X^{min}/R_X^{max} [m]	-4.2 / -0.3	
RMS_Y [m]	72.6	
R_Y^{min}/R_Y^{max} [m]	69.3 / 74.6	
RMS_Z [m]	25.9	
R_Z^{min}/R_Z^{max} [m]	-18.2 / -33.0	
s_0	22.46	

Table 3. Results of forward intersection with the original RPCs.

	Shift		Shift + Drift		Affine	
Scene	Fore	Aft	Fore	Aft	Fore	Aft
RMS_x [pixel]	0.25	0.26	0.25	0.26	0.25	0.26
RMS_y [pixel]	0.78	0.44	0.74	0.46	0.52	0.40
RMS_X [m]	0.66		0.66		0.65	
R_X^{min}/R_X^{max} [m]	-1.4 / 2.3		-1.3 / 2.3		-1.3 / 2.3	
RMS_Y [m]	1.12		1.16		0.95	
R_Y^{min}/R_Y^{max} [m]	-3.3 / 2.0		-4.3 / 2.9		-3.6 / 2.3	
RMS_Z [m]	2.23		1.99		1.67	
R_Z^{min}/R_Z^{max} [m]	-6.6 / 8.2		-4.8 / 7.5		-4.4 / 6.8	
s_0	0.59		0.47		0.38	

Table 4. Georeferencing results with bias corrected RPCs.

To assess the applicability of the RPC bias correction with minimal ground control information, two scenarios were tested. Adjustment was carried out using one GCP and bias correction by shifts, and also using three GCPs and bias correction by shifts and drifts. The results are summarized in Table 5.

In the case of only one GCP used to determine a bias correction by shifts, the RMS errors of object coordinates were around 1.6 m in planimetry and 2.4 m in height. Use of three GCPs and RPC bias correction by shifts and drifts resulted in RMS errors of 1.7 m in planimetry and 2.3 m in height. Use of minimal GCP information for the bias correction did not yield the same accuracy levels as shown in Table 4, but still demonstrated that precise georeferencing is possible even when only a few GCPs are available.

	Shifts / 1 GCP		Shifts + drifts / 3 GCPs	
Scene	Fore	Aft	Fore	Aft
RMS_x [pixel]	0.46	0.47	0.27	0.28
RMS_y [pixel]	0.79	0.46	1.03	0.62
RMS_X [m]	1.17		0.77	
R_X^{min}/R_X^{max} [m]	-2.5 / 1.3		-1.1 / 2.7	
RMS_Y [m]	1.11		1.61	
R_Y^{min}/R_Y^{max} [m]	-3.3 / 2.1		-4.7 / 4.8	
RMS_Z [m]	2.44		2.24	
R_Z^{min}/R_Z^{max} [m]	-8.3 / 6.5		-5.4 / 5.5	
s_0	0.38		0.35	

Table 5. RPC adjustment results using one and three GCPs.

4.3 Results using the generic pushbroom sensor model

Two variants of bundle adjustment were carried out, one using 9 GCPs and one using 15 GCPs. The results are shown in Table 6. There is little difference in the results, with those achieved using 9 GCPs being slightly better. In both cases the RMS errors of differences in image space were between 0.2 and 0.6 pixels, and the RMS errors of object coordinates were in the order of 1.6 m in planimetry and 1.4 m in height.

	9 control points		15 control points	
Scene	Fore	Aft	Fore	Aft
RMS_x [pixel]	0.27	0.30	0.27	0.27
RMS_y [pixel]	0.54	0.41	0.59	0.42
RMS_X [m]	1.29		1.29	
R_X^{min}/R_X^{max} [m]	-5.6 / 2.7		-5.8 / 1.5	
RMS_Y [m]	0.81		0.91	
R_Y^{min}/R_Y^{max} [m]	-2.1 / 3.3		-1.8 / 3.3	
RMS_Z [m]	1.35		1.45	
R_Z^{min}/R_Z^{max} [m]	-5.6 / 2.9		-5.9 / 2.5	
s_0	0.38		0.44	

Table 6. Georeferencing results with the generic pushbroom sensor model.

4.4 Discussion

The georeferencing results obtained for CARTOSAT 1 in the Hobart test field are very encouraging. Whereas direct georeferencing using the RPCs provided by ISRO yielded sub-optimal results, the provision of a small number of GCPs was enough to boost the positioning accuracy to subpixel level in planimetry and to slightly better than 1 pixel in height. Bias-corrected RPCs produced slightly higher accuracy than the 3D affine model in the case where the biases were modelled by an affine transformation. The generic pushbroom sensor model also achieved subpixel accuracy, almost independent from the number of GCPs used in the adjustment. The RMS errors in object space showed a different distribution than for bias corrected RPCs due to the different definitions of the coordinates, but the overall accuracy achieved was very similar. The interpretation of the results is somewhat limited by the fact that the distribution of the points in the test field was not optimal, since they covered only about one quarter of the scene.

5. CONCLUSION

This paper has described the successful application of three different sensor models to a panchromatic stereo pair from the CARTOSAT 1 satellite. The software package *Barista* was used to process the data. Geopositioning was carried out using the 3D affine model, bias corrected RPCs, and a generic pushbroom sensor model, and the results were used to assess the accuracy of geopositioning that can be achieved for CARTOSAT 1 imagery. It was shown that precise, sub-pixel geopositioning is possible with all three sensor models in situations where only a small number of GCPs are available.

REFERENCES

Barista, 2008. Barista product information webpage, http://www.baristasoftware.com.au (accessed 08 Feb. 2008).

Cartosat 1a, 2006. Data User's Handbook, India, http://www.nrsa.gov.in/Cartosat-1handbook.html, (accessed 08 Feb. 2008).

Cartosat 1b, 2006. Brochure, India, http://www.nrsa.gov.in/cartosat-1broch.html (accessed 08 Feb. 2008).

Fraser, C., Dial, G., Grodecki, J., 2006. Sensor orientation via RPCs. *ISPRS Journal of Photogrammetry & Remote Sensing* 60(3): 182-194.

Fraser, C., Hanley H., 2003. Bias compensation in rational functions for IKONOS satellite imagery. *PE&RS* 69(1): 53-57.
Fraser, C., Hanley, H., 2005. Bias-compensated RPCs for sensor orientation of high-resolution satellite imagery. *PE&RS* 71(8): 909-916.

Grodecki, J. and Dial, G., 2001. IKONOS geometric accuracy. *Proc. ISPRS Workshop: High-Resolution Mapping from Space, Hanover, Germany*, 8 pp. (on CD ROM).

Hanley, H., Yamakawa, T., Fraser, C., 2002. Sensor orientation for high-resolution satellite imagery. *International Archives of Photogrammetry and Remote Sensing* XXXIV / 1, pp. 69-75.

Tao, V., Hu, Y., 2002. 3D reconstruction methods based on the rational function model. *PE&RS* 68(7): 705-714.

Weser, T., Rottensteiner, F., Willneff, J., Fraser, C., 2007. A generic pushbroom sensor model for high-resolution satellite imagery applied to SPOT 5, QuickBird and ALOS data sets, *Proc. ISPRS Workshop: High-Resolution Mapping from Space, Hanover, Germany*, 6 pp (on CD ROM).

Yamakawa, T., Fraser, C., 2004. The affine projection model for sensor orientation: experiences with high-resolution satellite imagery. *International Archives of Photogrammetry and Remote Sensing*, XXXV / B1, pp. 142-147.

ACKNOWLEDGEMENTS

The image data set of Hobart was provided by the Indian Space Research Organisation (ISRO). The authors want to thank the image providers for supplying their data sets to make the analyses reported in this paper possible. Special thanks go to Mr. Zaffar Sadiq of Satellite Data Australia Pty Ltd and Dr. CVS Prakash of Antrix (ISRO), who helped to provide the unencrypted RPCs.